submitted to the *Astronomical Journal* 15 JUNE 2010

The Solar Neighborhood. XXII. Parallax Results from the CTIOPI 0.9m Program: Trigonometric Parallaxes of 64 Nearby Systems with $0\farcs5 \leq \mu \leq 1\farcs0$ yr^{-1} (SLOWMO sample)

Adric R. Riedel[1]

Department of Physics and Astronomy, Georgia State University, Atlanta, GA 30302-4106

riedel@chara.gsu.edu

John P. Subasavage[1]

Cerro Tololo Inter-american Observatory, La Serena, Chile

jsubasavage@ctio.noao.edu

Charlie T. Finch[1]

Astrometry Department, U.S. Naval Observatory, Washington DC 20392

finch@usno.navy.mil

Wei Chun Jao[1], Todd J. Henry[1], Jennifer G. Winters[1], Misty A. Brown[1]

Department of Physics and Astronomy, Georgia State University, Atlanta, GA 30302-4106

jao@chara.gsu.edu, thenry@chara.gsu.edu, winters@chara.gsu.edu, brown@chara.gsu.edu

Philip A. Ianna[1]

Department of Astronomy, University of Virginia, Charlottesville, VA 22904

pai@virginia.edu

Edgardo Costa[1], Rene A. Mendez[1]

Departamento de Astronomia, Universidad de Chile, Santiago, Chile

costa@das.uchile.cl, rmendez@das.uchile.cl

ABSTRACT

We present trigonometric parallaxes of 64 stellar systems with proper motions between $0\farcs5$ yr^{-1} and $1\farcs0$ yr^{-1} from the ongoing RECONS (Research Consortium On Nearby Stars) parallax program at CTIO (the Cerro Tololo Interamerican Observatory). All of the systems are south of DEC = +30, and 58 had no previous trigonometric parallaxes. In addition to parallaxes for the systems, we present proper motions, Johnson-Kron-Cousins VRI photometry, variability measurements, and spectral types. Nine of the systems are multiple; we present results for their components, three of which are new astrometric detections. Of the 64 systems, 56 are within 25 parsecs of the Sun and 52 of those are in the southern hemisphere, comprising 5.7% of the total number of known southern 25 parsec systems.

1. Introduction

One of the most important products of nearby star research will be a volume-limited sample of nearby stars. All-inclusive volume-limited samples of stars will allow us to answer large numbers of questions about the formation, kinematics, stellar mass fraction, and metallicity distributions of stars and (if representative) the galaxy itself. Due to the faintness of the M dwarfs that make up *at least* 72% of all nearby stars, surveys aiming at completeness are easiest carried out near the Sun. Large numbers of potential nearby stars have been found in ongoing series of proper motion surveys, most notably (among others too numerous to mention here) the surveys of Luyten (Luyten 1979), Giclas (Giclas 1958), Pokorny (Pokorny et al. 2003), ourselves (Subasavage et al. 2005), and Lepine (Lépine 2005). Various other surveys (for instance, Reylé & Robin 2004; Reid et al. 2008; Jahreiß et al. 2008) have followed up on those discoveries with spectroscopy and photometry to determine distances and spectral properties of these systems, although a great many still remain uninvestigated. For our purposes, however, we need accurate distances to prove membership, obtain accurate luminosities, and good kinematics.

While there are many methods used to determine stellar distances, the most accurate method remains the trigonometric parallax. It does not rely on any prior knowledge about the star (as photometric and spectroscopic "parallaxes" do), nor does it require a cluster

[1]Visiting Astronomer, Cerro Tololo Inter-american Observatory. CTIO is operated by AURA, Inc. under contract to the National Science Foundation.

of stars (as secular and statistical parallax do), nor a companion (as orbital parallax does). Trigonometric parallax is a geometric process, involving only the Earth's orbital motion and the distance to the star, operating independently of any unusual or misleading properties a star might have.

The primary compendia of trigonometric parallaxes are the General Catalog of Trigonometric Stellar Parallaxes, Fourth Edition (van Altena et al. 1995), more commonly known as the Yale Parallax Catalog (YPC), and the *Hipparcos* mission (Perryman et al. 1997). The YPC is a compilation of 15994 parallax measurements for 8112 stars from various observatories, representing ground-based parallax efforts prior to 1995 for stars as faint as $V = 21.5$. The parallaxes have a broad range of errors, but most are between 2 and 20 milliarcseconds (mas), as shown in Figure 1. The latest version of the *Hipparcos* mission's catalog (van Leeuwen 2007) contains 117955 stellar parallaxes, generally with errors less than 1 mas for stars brighter than $V = 8$. These compendia have already enabled statistical studies of stellar formation, evolution, composition, kinematics, and populations, making detailed large-scale surveys like the Geneva-Copenhagen Survey (Holmberg et al. 2009) of F and G dwarfs, for example, finally possible.

Despite the size of its catalog, *Hipparcos* did not find the complete population of nearby stars. The faint magnitude limit of *Hipparcos* was $V \sim 13$, with a completeness limit of $V \sim 7.3$ (Perryman et al. 1997). Populations of stellar types AFGK within 100 pc were richly sampled by *Hipparcos*, but intrinsically faint stars such as M dwarfs, cool subdwarfs, and white dwarfs largely remain the purview of the YPC, or of new ground-based efforts such as the one discussed here. A truly inclusive, volume-limited survey of all types of stars on the scale of the Geneva-Copenhagen survey is still not possible — large numbers of stars in the solar neighborhood are still unconfirmed, large numbers of M dwarfs are still missing from nearby star lists. [1]

The mission of RECONS (Research Consortium On Nearby Stars)[2] is to understand the solar neighborhood, including the discovery, confirmation, and characterization of nearby stars and their environments. RECONS has been operating a trigonometric parallax program called CTIOPI (Cerro Tololo Interamerican Observatory Parallax Investigation) at the CTIO 0.9m telescope since 1999 with a primary goal of pushing the parallax-verified solar neighborhood sample — systems within 25 pc, with a concentration on those within 10 pc — toward completion. This is the fifth paper of results from the ongoing program at the 0.9m, following Jao et al. (2005), Henry et al. (2006), Gizis et al. (2007), and Subasavage et al.

[1] updates at http://www.recons.org/census.posted.htm

[2] http://www.recons.org

(2009); more details of the program can be found in the preceding references.

While this paper does not finish off the sample of all stars in this proper motion range, it furthers the CTIOPI goal of completing the census of the solar neighborhood. It contains 67 new trigonometric parallaxes of 64 systems with proper motions between $0\farcs5$ yr^{-1} and $1\farcs0$ yr^{-1}, our "SLOWMO" sample. Of the 64 systems, 56 are within 25 pc of the Sun, and all are south of DEC= +30. In addition to the parallaxes, we provide new measurements of proper motions, Johnson-Kron-Cousins VRI photometry, variability, spectral types, and astrometric measurements of multiple systems.

2. The Sample

Completing the stellar census within 25 pc is a daunting task. If we assume the current census of systems within 5 pc is accurate (50 systems,[3] see Henry et al. (2006) for the most recent additions within five pc) and representative of the stellar space density of the solar neighborhood, we expect 6250 star systems within 25 pc. The most complete parallax-selected list of objects remains the NStars Database, which includes only 2011 systems within 25 pc (Henry et al. 2002), indicating that the sample is only 32% complete. Clearly, much more work is needed to achieve a truly comprehensive volume-limited sample of space; only then will we truly be able to characterize the compositional nature of the Galaxy. Even the Gaia mission, with a limiting magnitude of $V = 20$, will not reach the end of the main sequence past ten parsecs.

The 64 systems discussed in this paper are listed in Tables 1 and 2. They were selected for the CTIOPI program for a variety of reasons: either their high proper motion made them targets for M. Brown's masters thesis on SLOWMO systems, their estimated distances suggested they might be within 10 parsecs, or they had YPC parallaxes with large errors that placed the system within 10 parsecs. The systems themselves are all from Luyten (1979), Luyten (1957), Wroblewski & Torres (1991), Wroblewski & Torres (1994), Scholz et al. (2000), and a private communications with Scholz (1999) for APMPM J2127-3844. Most of them were investigated for companions in Jao et al. (2003). All of the systems have proper motions of $0\farcs5$–$1\farcs0$ yr^{-1}, have red dwarf primaries with $V = 10.35$–19.17 and have spectral types M1.0V to M6.0V. Seven of the systems presented here have known or suspected companions; we confirm six of them and present individual parallax measurements for components of three. We have also discovered evidence of multiplicity for a further three systems and suspect additional components in five more systems; thus 14% (9 out of 64) of

[3]http://www.recons.org/TOP100.posted.htm

our systems are multiple, and 9% (5 out of 64) are suspected multiples.

This sample builds upon our previous efforts that also revealed systems within 25 pc, including stars with $\mu \geq 1\farcs0$ yr^{-1} (Jao et al. 2005) (our MOTION sample), red dwarfs within 10 pc (Henry et al. 2006), and white dwarfs within 25 pc (Subasavage et al. 2009) from the CTIOPI 0.9m program, and mixed samples from our 1.5m program (Costa et al. 2005, 2006).

3. Observations

3.1. Astrometric and Photometric Observations

All astrometric and photometric observations were carried out at the CTIO 0.9m telescope, initially (1999-2003) under the aegis of the NOAO (National Optical Astronomy Observatory) Surveys Program, and later (2003-present) via the SMARTS (Small and Moderate Aperture Research Telescope System) Consortium. The observations presented in this paper were obtained between 1999 and 2009 utilizing the center 1024x1024 pixels of the 0.9m telescope's Tek 2048x2046 CCD and CTIO's V_J, R_{KC}, and I_{KC} (hereafter without subscripts)[4] filters. Additional details of the observing protocol can be found in Jao et al. (2005).

Four significant instrumental events in the course of the CTIOPI program have affected data published in this paper:

- In February 2005, the Tektronix #2 V filter (hereafter "old V") used by CTIOPI cracked and was replaced by the almost-photometrically identical (transmission properties and bandwidth) Tektronix #1 V filter (hereafter "new V"). With four years of new V data, we are able to make some comparisons between the two:

  As reported in Subasavage et al. (2009), the new V filter is photometrically consistent with the old V filter to within reported CTIOPI accuracies (0.03 mag, Henry et al. 2004), although we find our V filter photometry is only accurate to 0.05 mag in this dataset.

  Also as reported in Subasavage et al. (2009), some new V filter data cause a few-mas offset in the RA axis astrometric residuals. This is endemic to the new V filter itself and is not the result of changing filters; recent data taken with the old V filter show no such behavior in the residuals when added to older data. Parallax results using

[4]Subscripts: "J" indicates Johnson, and "KC" indicates Kron-Cousins. The central wavelengths for V_J, R_{KC}, and I_{KC} are 5475, 6425, and 8075 Å, respectively.

only new V filter data are slightly but non-systematically displaced relative to results using only old V data, which were found to be consistent with YPC and *Hipparcos* parallaxes in Jao et al. (2005). Part of the error appears to depend on the filter itself, the rest appears to depend on coverage: tests were only conducted on stars with large datasets before and after the V filter replacement. Those stars tend to have better coverage of the parallax ellipse in old V (earlier) than in new V (later, when their parallaxes were well determined and they became lower priority targets). Even so, the new V parallax is usually within 2-σ of the old V measurement, and mixed V parallaxes are always within 2-σ. All parallaxes in this paper using new V filter data are noted in Table 1.

- In April 2005, the Telescope Control System (TCS) on the 0.9m was completely replaced and refurbished, yielding improved pointing and tracking. No astrometric effects have been detected in datasets spanning the TCS upgrade.

- On 7 March 2009, a power outage damaged the gain = 1 circuitry for the CCD, and CTIOPI began using gain = 2. The differences between the two gains are purely electrical, and tests confirm that the switch does not affect our astrometry, as expected.

- In July 2009, the old V filter was returned to service. Extensive tests showed the hairline crack near the edge does not affect data acquired on the central quarter of the CCD as used in CTIOPI. Furthermore, testing many stellar fields indicated no adverse effects on the astrometry when reducing data with and without recent data in the old V filter. Recent old V filter data have been used in this paper's astrometric reductions of LHS 1050, LHS 1561, LHS 3443, LHS 4009AB, and LHS 4016.

3.2. Spectroscopic Observations

We carried out spectroscopic observations at two telescopes to determine the spectral types of 25 of the objects listed in Table 2. From 2003–2006, we used the CTIO 1.5m, the R-C Spectrograph with a Loral 1200 × 800 CCD, and the 32/I grating to obtain spectra covering 6000–9500Å at a resolution of 8.6Å. For WT 244 and GJ 438, we used the CTIO 4m, the R-C spectrograph with a Loral 3X × 1K CCD, and the 181 grating to obtain spectra covering 5500–10000Å at a resolution of 5.7Å. Further details concerning the 1.5m spectroscopy program and associated data reduction can be found in Henry et al. (2004), while details of the 4m spectroscopy program can be found in Henry et al. (2002).

4. Results

4.1. Astrometry — Parallaxes and Proper Motions

Parallaxes and proper motions of 64 stellar systems are presented in Table 1. Nine of our systems have multiple parallax measurements, from YPC, our CTIOPI 1.5m program, or multiple components published in this paper. For these cases, we present weighted average system parallaxes in Table 3.

All parallax data were analyzed with the custom IRAF/IDL pipeline used in CTIOPI publications since 2005, using an iterative Gaussfit program described in Jao et al. (2005). Starting in 2007, the reduction methodology was changed by the implementation of a new SExtractor centroiding algorithm, described in Subasavage et al. (2009).

As always, CTIOPI parallaxes must meet several criteria before they are deemed fit to publish. First, to ensure good coverage of the parallax ellipse, there is an informal limit of 30 frames each in the 'morning' and 'evening' halves of the ellipse with a goal of having 20 usable frames each; the number of frames used in the final reductions ranged from 45 (LHS 2899) to 137 (LHS 1630AB). Second, the system must be followed for about two years to decouple the star's motion into parallax and proper motion; the coverage in this paper varies from 1.99 years (LHS 2335) to 10.15 years (LHS 4009AB). Third, CTIOPI targets are expected to have parallax errors less than 3 mas before publishing. The smallest parallax error we are publishing here is 0.63 mas (GJ 1157) and the largest is 2.57 mas (LHS 1050 and LHS 2122), while the median error on these parallaxes is 1.37 mas.

Our parallaxes are derived by measuring the motion of the target star (pi star) relative to background reference stars, and then correcting the parallactic motion to an absolute reference frame with VRI band photometric distance estimates to the reference star ensemble (not to be confused with our $VRIJHK$ distance estimates for red dwarfs, discussed in §4.6). Good reference star fields consist of at least five but rarely more than twelve stars that are as close as possible to the pi star on the CCD, have more than 1000 peak counts, and surround the pi star as much as possible. The most accurate parallaxes are obtained with exposures longer than 90 seconds, which is long enough at CTIO for images in the VRI bands to smooth over atmospheric effects and consequently improve centroids. We have also re-observed several systems (e.g. LHS 1561, LHS 3909, and LHS 3443) after a multi-year hiatus to improve proper motions and possibly reveal long-period perturbations (see §4.3), otherwise the extra observations have a minor effect on the derived parallax.

4.2. Astrometry — Multiples

Seven of our systems contain known multiples: LHS 1630AB, LHS 1749AB, LHS 1955AB, LHS 2567/2568, LHS 3001/3002, LHS 3739/3738AB, and LHS 4009AB. We have resolved orbital motion above the 3-σ level (angular motion or changes in separation) for five of those systems, as described in Table 4. Apart from LHS 1955AB, all values published in Table 4 are derived from at least three frames on the nights listed.

The components of LHS 1630AB, LHS 1749AB and LHS 1955AB are close enough that their PSFs (point spread functions) overlap. In the case of LHS 1630AB the B component was never fully resolved, but it does appear as an elongation to the PSF. LHS 1749AB was only resolved on 15 frames from four nights. LHS 1955AB was only resolved on seven frames from five nights using restricted centroiding parameters that enabled the separation of blended sources; the two frames from the earliest night and the one frame from the latest night are used to derive the results in Table 4.

Errors presented in Table 4 include both measurement and systematic errors. The systematic errors were computed from the nights of data measured for Table 4, with the exception of the three frames used for LHS 1955AB. All frames from a single visit (one night of observations on one system) were compared to the 2MASS All-Sky Point Source Catalog using *imwcs* [5]; the standard deviations of the plate scales and rotations per-visit were then averaged across all visits to get a more representative error. Systematics for the CTIO 0.9m on those frames give a 0.015% error in the plate scale (and therefore separations), and a 0.0083 degree error in the rotation (and therefore position angles). In all cases, the measurement errors dominate the systematic errors.

4.3. Astrometry — New astrometric multiples

Three of the systems discussed here — LHS 1582AB, LHS 2071AB, and LHS 3738AB — have been found to be previously undetected astrometric binaries, as shown in Figures 2, 3, and 4, respectively. For comparison, three additional stars — LHS 2021, LHS 3739 and LHS 4009AB — are shown in Figures 5, 4 and 6. LHS 2021 and LHS 3739 appear to be single stars while LHS 4009AB is a known close binary that also appears single in our data. We re-observed LHS 4009AB several years after the parallax was finished to search for long-term perturbations; none was found. All five systems are discussed in detail in §5.

[5]A World Coordinate System setting program from the WCSTools library, http://tdc-www.harvard.edu/software/wcstools/

The CTIOPI parallax reduction pipeline fits the astrometric positions of a star to a linear proper motion and a parallax ellipse of known shape and unknown size. Any further motion caused by the orbit of a companion remains, appearing as a perturbation in the astrometric residuals. Unlike an orbit determined by a technique that resolves two objects in a binary, an astrometric perturbation describes the orbit of the photocenter, not the motion of any individual component. (Astrometric perturbations are therefore greater for larger magnitude differences between the components, larger companion masses, and larger semi-major axes of the orbits; the photocenter of an equal-mass equal-luminosity binary will not move at all.) We can still solve for all orbital elements except semi-major axis. In its place, we can determine the semi-major axis of the photocentric orbit, which can then be scaled to the relative orbit if the system is resolved.

Photocentric orbital elements for the three new astrometric binaries were computed from the astrometric residuals using an iterative Thiele-Innes least-squares solver (Hartkopf et al. 1989) and are given in Table 5. Points from nights with only a single CCD image (generally obtained for the purpose of photometry) were removed. The orbits should be considered preliminary, as our astrometric datasets do not have sufficient time coverage to publish definitive orbits, particularly in the case of LHS 2071AB for which the orbit is not complete. LHS 2071AB and LHS 3738AB have now both been resolved through followup work, as discussed in §5.

The parallaxes published in Table 1 were computed from data where the photocentric orbit was removed. The orbital position of the photocenter was calculated and subtracted from the actual measured position of the photocenter at each data point, including those from nights with only a single CCD image. The parallax was then re-reduced based on this new dataset.

CTIOPI's detection capabilities are limited by several factors. Systems are typically observed 1–4 times a year and thus the data are insensitive to periods less than a year. The program has only been running for ten years, and cannot wrap orbits with periods longer than ten years. CTIOPI also has a 3–6 mas nightly precision error (depending on the specifics of the reference field) that limits our sensitivity to low-amplitude binaries. Fortunately, astrometric perturbations are typically self-confirming; genuine orbital motion will show up in both the RA and DEC axes unless the orbit is nearly north-south or east-west on the sky. Nevertheless, to check for systematics within the field we have reduced the three brightest reference stars in each of our astrometric perturbation fields as if they were the parallax target. In only one case did a reference star showed a perturbation of any kind; that reference was removed from the reduction of LHS 2071AB.

4.4. Photometry — Variability

The variability values in Table 2 are calculated according to the methodology of Honeycutt (1992) with additional details given in Henry et al. (2006). In Table 2 we list the level of variability in magnitudes (Column 8) of each target star in its parallax filter (Column 7). The number of nights on which each star was observed (Column 9) and the number of frames (Column 10) used for the variability study are also given.

Although many M dwarfs are minutely variable, none of the stars in this sample have been found to vary by more than 2% in the frame series available. The single exception is LHS 1749AB at 0.028 mag. In this case, the variability is likely due to the B component at a separation of 3″ falling within the relative photometry aperture, and variations in seeing affecting the extracted fluxes.

4.5. Photometry — Standard

VRI magnitudes are listed in Table 2, along with extracted JHK_s magnitudes from the Two Micron All Sky Survey Catalog of Point Sources (Skrutskie et al. 2006). The errors on the VRI magnitudes are less than 0.05 mag for V, and 0.03 mag for R and I, with few exceptions, most notably the faint stars LHS 2021 and LHS 3002. All photometric observations were reduced via a custom IRAF pipeline and transformed onto a the Johnson-Kron-Cousins system through the use of photometric standards from Landolt (1992), Landolt (2007) and Graham (1982), as described in Henry et al. (2006).

4.6. Photometry — Distance Estimates

For purposes of initial target selection as well as for additional analysis once trigonometric distances are determined, we used our CCD photometry combined with 2MASS JHK photometry to calculate the photometric distances listed in Table 2 (Columns 16 and 17). The fourth-order polynomial fits for twelve color-absolute magnitude relations, the process by which the relations were determined, and the calculation of internal and external errors are described in detail in Henry et al. (2004). Our quoted photometric distances have internal errors (defined as the standard deviation of the distances estimated from the twelve relations) below 10% and an additional external systematic error of 15.3%. The distribution of internal errors is shown in Figure 7; the average error is 3.9%, which is much smaller than the external errors. The errors listed for the photometric distances given in Table 2 include both internal and external errors.

Because the fits used for the photometric distance estimates are derived using main sequence stars, the estimates are only accurate when the objects are single, main-sequence, M dwarfs. For the most part, these systems are indeed single, and 54 of the 64 systems (84%) fall within the 2-σ range when their combined internal and external errors are considered, as shown in Figure 8. Stars above the 2-σ line in Figure 8 are likely to be underluminous subdwarfs, while those below the 2-σ line are presumably overluminous multiples. There are no subdwarfs in this sample, (although LHS 1050, LHS 1807, and LHS 3739/3738AB may be slightly metal-poor) but there are several known close multiples with combined photometry, either previously known (LHS 1630AB, LHS 1955AB, LHS 4009AB), or discovered by us (LHS 1582AB, LHS 2071AB, LHS 3738AB). There is considerable scatter in M_V along the main sequence, visible in Figure 9, with up to two full magnitudes of spread for early to mid M dwarfs. An equal magnitude binary will have a distance estimated to be 41% closer via photometry than is determined trigonometrically, but given the spread in M_V in the main sequence, only further work will confirm or refute the multiplicity of suspected targets.

4.7. Spectral Typing

Spectral types are given in Table 2, and come from five sources that can be arranged into two broad groups. One group is from RECONS spectroscopy, detailed in Kirkpatrick et al. (1991), Henry et al. (1994), and Henry et al. (2002). RECONS spectroscopy was used to determine the spectral types of all stars not taken from literature, and by Kirkpatrick et al. (1995) to classify LHS 1807.

The remaining spectral types are from the Palomar/Michigan State University Nearby Star Spectroscopic Survey (PMSU) (Reid et al. 1995; Hawley et al. 1996) and related paper Reid et al. (2007), all of which use the same weighted spectral indicies method linked to the spectral standards in Kirkpatrick et al. (1991). Where RECONS classifications were done over a range of 6000–9000Å with an effective resolution of 5.7–8.6Å depending on the setup (§3.2), the PMSU program used 6200–7500Å with resolution 1.8Å. In practice our results differ from PMSU results only occasionally and never more than half a subtype (see Table 6 for a comparison).

5. Systems Worthy of Note

LHS 1050: A 1.3-σ underluminous single-star system (11.7±0.3 pc trig/15.2±2.4 pc phot dist) that still appears to be on the main sequence as shown in Figure 9. The YPC

distance 11.5±1.8 pc is consistent with our distance, 11.7±0.3 pc. A weighted mean parallax is given in Table 3.

LHS 1561: The most overluminous system in the sample, it has a 4.4-σ distance mismatch (29.2±1.5 pc trig/13.5±2.1 pc phot dist, see Figure 8), and is noticeably elevated above the main sequence in Figure 9. We see no astrometric perturbation; it may be a multiple CTIOPI is not sensitive to or a pre-main-sequence object. The parallax has not 'stabilized': additional data continue to change the answer by more than 1-σ, which is often a sign of unresolved orbital motion.

LHS 1582AB: A new astrometric binary with a 6.4 yr period and an 18 mas photocentric semi-major axis (see Figure 2). It has a 2.7-σ distance mismatch (21.1±0.7 pc/13.3±2.3 pc phot dist, see Figure 8) and is elevated above the main sequence in Figure 9. A preliminary orbit is given in Table 5; the orbital motion was removed from the data before fitting the final parallax.

LHS 1630AB: We confirm the Adaptive Optics companion reported in Beuzit et al. (2004) seen on 18 September 2002 with a separation of 0.″61 at a position angle of 72 deg. The B component is visible in I band photometry frames as of 2007, as shown in Figure 10. The system has a 2.8-σ distance mismatch (17.8±0.3 pc trig/11.7±1.8 pc phot dist) and is elevated above the main sequence as seen in Figure 9, but we see no astrometric perturbation.

LHS 1749AB: A close visual binary discovered by Jao et al. (2003) with a separation of 2.″9 at a position angle of 140 deg (see Table 4). The parallax in Table 1 was calculated for the A component only, and that distance (21.7±0.7 pc) is consistent with 22.0±2.5 pc reported by the CTIOPI 1.5m program (Costa et al. 2006). A weighted mean parallax for the system is given in Table 3.

The B component is ∼2.8 mag fainter in V than A, as shown in Figure 11. LHS 1749B is separable from A on 15 parallax frames; the resulting relative parallax result is 43.17±4.33 mas (23.2±2.3 pc) which is of poor quality but consistent with other measurements. Evidence for orbital motion is shown in Table 4.

LHS 1807: A 1.5-σ underluminous system (14.1±0.3 pc trig/19.1±3.0 pc phot dist), but still evidently a main sequence star (see Figure 9).

LHS 1955AB: A close visual binary listed in Luyten (1979) with a 0.″8 separation at an angle of 290 deg. Our astrometric reduction uses relaxed ellipticity constraints (60%, not 20%) to keep frames where B extends the PSF of A. The B component is within the photometric aperture and causes the 3.1-σ overluminosity (13.5±0.2 pc trig/8.6±1.4 pc phot

dist) and the elevation above the main sequence seen in Figure 9. We detect no astrometric perturbation of A despite the motion of the B component.

LHS 1955B is ∼0.5 magnitudes fainter in R than A, and separable from A on only seven frames over five nights using special SExtractor settings. Using those frames, we can obtain a relative parallax for B: 73.65±19.58 mas (13.58±3.61 pc), consistent with the relative parallax of A in Table 1, 72.76±1.09 mas (13.74±0.21 pc). Considerable orbital motion can be seen in Figure 12 and Table 4 suggesting P∼80 yr. All results for B are questionable due to severe PSF contamination.

LHS 2010: This system has a 3.0-σ distance mismatch (13.7±0.3 pc trig/8.9±1.4 pc phot dist) and is elevated above the main sequence in Figure 9. We see no astrometric perturbation, but it may be a multiple to which CTIOPI is not sensitive.

LHS 2021: Contains the lowest luminosity star in our sample: $V = 19.17$, spectral type M6.0V (despite unusually red colors), which can be seen in the lower right of Figure 9. This paper's distance (15.7±0.3 pc) is consistent with the 16.7±1.3 pc distance reported by the CTIOPI 1.5m program in (Costa et al. 2006). A weighted mean system parallax is given in Table 3. This system is plotted as an example of single-star astrometric residuals in Figure 5.

LHS 2071AB: A new astrometric binary with P>9 years and a 21 mas photocentric semi-major axis (see Figure 3). The unseen companion is causing a 2.2-σ overluminosity (15.0±0.3 pc trig/10.8±1.7 pc phot dist, see Figure 8) and a noticeable elevation above the main sequence in Figure 9. The system has been resolved with adaptive optics on Gemini North; further results will follow in a later paper. An orbit consistent with our current dataset is given in Table 5, the orbital motion was removed from the data before fitting the final parallax.

LHS 5156: The final parallax is entirely based on new V filter data due to insufficient old V coverage. Our reduction does not show the characteristic new V wobble (§3.1) in the residuals, but it may be inaccurate by more than 1-σ.

GJ 438: The hottest and most luminous star in the sample, as can be seen in Figure 9. The YPC distance (8.4±1.1 pc) is inconsistent with our distance, 10.9±0.3 pc. This system is not in the RECONS 10 parsec sample. A weighted mean parallax to this system is given in Table 3.

LHS 2520: The third-most overluminous system in this sample; it has a 3.2-σ distance mismatch (12.8±0.4 pc trig/7.6±1.2 pc phot dist, see Figure 8) and is elevated above the main sequence as shown in Figure 9. We detect no astrometric perturbation; it may be a

multiple to which CTIOPI is not sensitive.

LHS 2567/2568: A visual binary with a separation of 8.″0 at a position angle of 61 deg (see Table 4). The A component (LHS 2567) has a 2.7-σ distance mismatch (21.4±0.8 pc trig/13.6±2.1 pc phot dist, see Figure 8) while the B component (LHS 2568) distance matches to 0.4-σ (20.6±0.8 pc trig/19.0±2.9 pc phot dist). LHS 2567 shows no astrometric perturbation, but given that it should be the same age and metallicity as LHS 2568, it is potentially an unresolved binary much like LHS 4009AB, below. The proper motions of A and B are discrepant by 11.1-σ due to orbital motion presented in Table 4. A weighted system parallax is given in Table 3.

LHS 3001/3002: A visual binary with a separation of 12.″7 at a position angle of 43.9 deg (see Table 4). The B component (LHS 3002) is the second-coolest star in this sample, as shown in Figure 9. The proper motions of A and B are discrepant by 4.8-σ due to orbital motion presented in Table 4. A weighted system parallax is given in Table 3.

LHS 3080: The second-most overluminous system in this sample. It has a 3.2-σ distance mismatch system (28.2±1.5 pc trig/15.7±2.4 pc phot dist, see Figure 8) and is elevated above the main sequence as shown in Figure 9. We detect no astrometric perturbation; it may be a multiple to which CTIOPI is not sensitive.

LHS 3197: We have used an average correction to absolute parallax (1.50±0.50 mas) for this system because the calculated correction (3.44 mas) was abnormally large. This is likely due to artificial reddening of the reference stars, caused by the molecular cloud LDN 1781 (Lynds 1962), which (if circular) has radius 37′ and a center only 22′ away at a position angle of 43 deg.

GJ 633: The published YPC distance (9.6±1.3 pc) is inconsistent with our distance, 16.8±0.3 pc, which supersedes the 22.5 pc±0.9 pc distance published by us in Henry et al. (2006). Improvements in centroiding discussed in §4.1 now reliably distinguish GJ 633 from a point source 7″ away that contaminated the previous result. The system is still not in the RECONS 10 parsec sample. A weighted mean system parallax (this new result and YPC) is given in Table 3.

WT 562: Unrelated to the system SCR 1826-6542 (Finch et al. 2007), 5.′8 away. WT 562 has $\mu = 0.''611$ yr^{-1} at 180.9 deg while SCR 1826-6542 has $\mu = 0.''311$ yr^{-1} at 178.9 deg. Early results also suggest SCR 1826-6542 is several parsecs closer.

LHS 3739/3738AB: A heirarchical triple system consisting of a new astrometric binary, LHS 3738AB, which is itself the B component of a known visual binary with LHS 3739. The system is the most underluminous in our sample. Using identical reference fields and

frames (see Figure 4), LHS 3739 has no signs of perturbation and is 1.6-σ *under*luminous (19.6±0.4 pc trig/27.6±4.5 pc phot dist, see Figure 8) while the light of the components of LHS 3738AB combine to give only a 0.3-σ (19.7±0.4 pc trig/18.5±3.0 pc phot dist) difference from expectations. Even so, LHS 3739 (and therefore LHS 3738 A and B) seems to be main-sequence in Figure 9.

The LHS 3739/LHS 3738AB visual binary has a separation of 113.″1 at a position angle of 95.7 deg, and has proper motions discrepant by 2.3-σ. This orbital motion is detected and presented in Table 4. A weighted system parallax is given in Table 3.

The LHS 3738AB new astrometric binary has a 5.8 year period and a 27 mas photocentric semi-major axis (see Figure 4), and has been resolved by Gemini North. A preliminary orbit is given in Table 5 and was removed from the data before fitting the final parallax. Further results will be published in a later paper.

LHS 4009AB: We do not confirm the companion from Montagnier et al. (2006) resolved with adaptive optics on 14 October 2005 with a separation of 0.″07 at a position angle of 250 deg, and $\Delta K = 0.15$ in what Montagnier et al. (2006) claim is a three year orbit. The system has a 1.9-σ distance mismatch (12.5±0.2 pc trig/9.2±1.5 pc phot dist) and is elevated above the main sequence, (see Figure 9) but we detect no astrometric perturbation (see Figure 6), probably because the system components are nearly equal luminosity in R.

LHS 4016: The system has a 2.0-σ distance mismatch (24.2±0.9 pc trig/17.2±2.7 pc phot dist, see Figure 8) and is elevated above the main sequence as shown in Figure 9. There are possible signs of an astrometric perturbation, but a gap from 2005 to 2009 when the old V filter was not used prevents any definite determination.

6. Discussion

As shown in Figure 1, our parallax errors compare favorably to the errors from other ground-based parallax efforts, as summarized in YPC. Our increased accuracy can be attributed to our use of CCD images for our astrometry, while most of the YPC parallaxes were measured from photographic plates.

In Figure 13 we plot the distribution of tangential velocities listed in Column 15 of Table 1. Most of the stars have v_{tan} = 25–100 km sec^{-1}, as expected for disk red dwarfs (Mihalas & Binney 1981). The single star with v_{tan} = 126 km sec^{-1} is LTT 5066, which at 46 pc is the furthest star discussed in this paper; by photometry and spectroscopy it is a dwarf, not a subdwarf. Our sample is kinematically biased, requiring stars to have $0.''5 \leq \mu \leq 1.''0$

yr^{-1}. As such, the nearest star, LHS 5156, must have a tangential velocity between 25 and 50 km sec^{-1}, while our farthest star, LTT 5066, could not be in our proper motion regime if it were moving any slower than 110 km sec^{-1}.

The 56 systems within 25 pc described here constitute 2.7% of all systems now confirmed by parallax to be in the 25 pc sample (5.7% of systems in the southern hemisphere), according to the statistics from the NStars Database (Henry et al. 2002), using 2011 previously known systems as a baseline. Including parallax results from the entire CTIOPI program, we have added 155 new systems (a 7.7% increase) to the all-sky 25 pc sample. Of those 25 pc systems, 142 are in the southern hemisphere, a net increase of 16.6% in the south alone. We are currently observing roughly a hundred additional systems that may prove to be within 25 pc, and continue to add more as observing time and stamina permit. Nonetheless, we do not anticipate completing the census of all systems in the solar neighborhood through CTIOPI alone, which means that ground-based sky survey efforts such as Pan-STARRS (The Panoramic Survey Telescope & Rapid Response System), SkyMapper, LSST (the Large Synoptic Survey Telescope), and space-based missions like Gaia, will undoubtedly reveal many more of the Sun's neighbors.

7. Acknowledgements

The RECONS effort is supported primarily by the National Science Foundation through grants AST 05-07711 and AST 09-08402, as well as through NASA's *Space Interferometry Mission*. Observations were initially made possible by NOAO's Survey Program and have continued via the SMARTS Consortium. This research has made use of results from the NStars Project, NASA's Astrophysics Data System Bibliographic Services, the SIMBAD and VizieR databases operated at CDS, Strasbourg, France, the SuperCOSMOS Sky Survey, and the 2MASS database.

The authors also wish to thank Mr. Sergio Dieterich for the Gemini observations and reductions; Dr. Brian Mason for supplying the orbit-fitting code; and the staff of the Cerro Tololo Inter-american Observatory, particularly Edgardo Cosgrove, Arturo Gomez, Alberto Miranda, and Joselino Vasquez for their help over the years. The authors also wish to thank Dr. Hugh Harris and Dr. Jennifer Bartlett for their constructive comments.

REFERENCES

Beuzit, J.-L., et al. 2004, A&A, 425, 997

Costa, E., Méndez, R. A., Jao, W.-C., Henry, T. J., Subasavage, J. P., Brown, M. A., Ianna, P. A., & Bartlett, J. 2005, AJ, 130, 337

Costa, E., Méndez, R. A., Jao, W.-C., Henry, T. J., Subasavage, J. P., & Ianna, P. A. 2006, AJ, 132, 1234

Finch, C. T., Henry, T. J., Subasavage, J. P., Jao, W.-C., & Hambly, N. C. 2007, AJ, 133, 2898

Giclas, H. L. 1958, Lowell Observatory Bulletin, 4, 1

Gizis, J. E., Jao, W.-C., Subasavage, J. P., & Henry, T. J. 2007, ApJ, 669, L45

Gliese, W., & Jahreiß, H. 1991, On: The Astronomical Data Center CD-ROM: Selected Astronomical Catalogs, Vol. I; L.E. Brotzmann, S.E. Gesser (eds.), NASA/Astronomical Data Center, Goddard Space Flight Center, Greenbelt, MD,

Graham, J. A. 1982, PASP, 94, 244

Hartkopf, W. I., McAlister, H. A., & Franz, O. G. 1989, AJ, 98, 1014

Hawley, S. L., Gizis, J. E., & Reid, I. N. 1996, AJ, 112, 2799

Henry, T. J., Kirkpatrick, J. D., & Simons, D. A. 1994, AJ, 108, 1437

Henry, T. J., Walkowicz, L. M., Barto, T. C., & Golimowski, D. A. 2002, AJ, 123, 2002

Henry, T. J., Subasavage, J. P., Brown, M. A., Beaulieu, T. D., Jao, W.-C., & Hambly, N. C. 2004, AJ, 128, 2460

Henry, T. J., Jao, W.-C., Subasavage, J. P., Beaulieu, T. D., Ianna, P. A., Costa, E., & Méndez, R. A. 2006, AJ, 132, 2360

Holmberg, J., Nordström, B., & Andersen, J. 2009, A&A, 501, 941

Honeycutt, R. K. 1992, PASP, 104, 435

Jahreiß, H., Meusinger, H., Scholz, R.-D., & Stecklum, B. 2008, A&A, 484, 575

Jao, W.-C., Henry, T. J., Subasavage, J. P., Bean, J. L., Costa, E., Ianna, P. A., & Méndez, R. A. 2003, AJ, 125, 332

Jao, W.-C., Henry, T. J., Subasavage, J. P., Brown, M. A., Ianna, P. A., Bartlett, J. L., Costa, E., & Méndez, R. A. 2005, AJ, 129, 1954

Kirkpatrick, J. D., Henry, T. J., & McCarthy, D. W., Jr. 1991, ApJS, 77, 417

Kirkpatrick, J. D., Henry, T. J., & Simons, D. A. 1995, AJ, 109, 797

Landolt, A. U. 1992, AJ, 104, 340

Landolt, A. U. 2007, AJ, 133, 2502

Lépine, S. 2005, AJ, 130, 1680

Luyten, W. J. 1957, Minneapolis, Lund Press, 1957.,

Luyten, W. J. 1979, LHS Catalogue. Second edition., by Luyten, W. J.. Publ. by Univ. Minnesota, Minneapolis, USA., 100 p.

Lynds, B. T. 1962, ApJS, 7, 1

Mihalas, D., & Binney, J. 1981, San Francisco, CA, W. H. Freeman and Co., 1981. 608 p.,

Montagnier, G., et al. 2006, A&A, 460, L19

Perryman, M. A. C., et al. 1997, A&A, 323, L49

Pokorny, R. S., Jones, H. R. A., & Hambly, N. C. 2003, A&A, 397, 575

Reid, I. N., Hawley, S. L., & Gizis, J. E. 1995, AJ, 110, 1838

Reid, I. N., Cruz, K. L., & Allen, P. R. 2007, AJ, 133, 2825

Reid, I. N., Cruz, K. L., Kirkpatrick, J. D., Allen, P. R., Mungall, F., Liebert, J., Lowrance, P., & Sweet, A. 2008, AJ, 136, 1290

Reylé, C., & Robin, A. C. 2004, A&A, 421, 643

Scholz, R.-D., 1999, private communication

Scholz, R.-D., Irwin, M., Ibata, R., Jahreiß, H., & Malkov, O. Y. 2000, A&A, 353, 958

Skrutskie, M. F., et al. 2006, AJ, 131, 1163

Subasavage, J. P., Henry, T. J., Hambly, N. C., Brown, M. A., Jao, W.-C., & Finch, C. T. 2005, AJ, 130, 1658

Subasavage, J. P., Jao, W.-C., Henry, T. J., Bergeron, P., Dufour, P., Ianna, P. A., Costa, E., & Méndez, R. A. 2009, AJ, 137, 4547

van Altena, W. F., Lee, J. T., & Hoffleit, E. D. 1995, New Haven, CT: Yale University Observatory, —c1995, 4th ed., completely revised and enlarged,

van Leeuwen, F. 2007, A&A, 474, 653

Wroblewski, H., & Torres, C. 1991, A&AS, 91, 129

Wroblewski, H., & Torres, C. 1994, A&AS, 105, 179

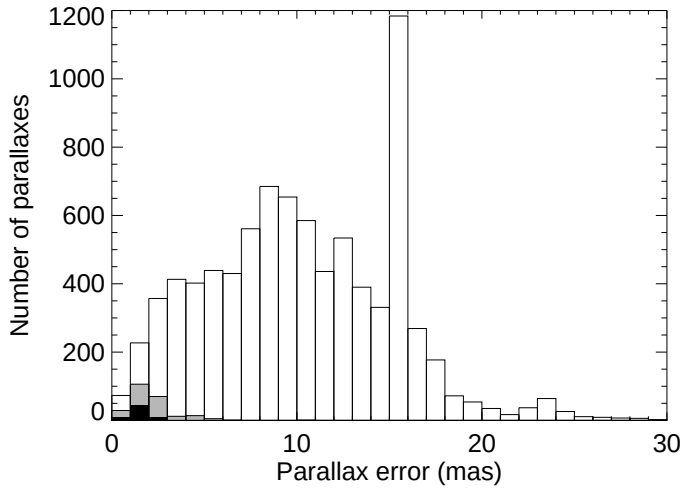

Fig. 1.— Parallax errors for systems in this paper (black), and previous CTIOPI parallax papers (gray) are shown versus previous ground-based parallaxes from YPC (white, extends off this graph). Our improved precision is due to our CCD-based astrometry while the bulk of previous work was done with photographic plates. A few systems in this paper are also in YPC (see Table 3). The enormous spike at 15 mas is a result of the methods used in YPC to assign errors to parallaxes published without error.

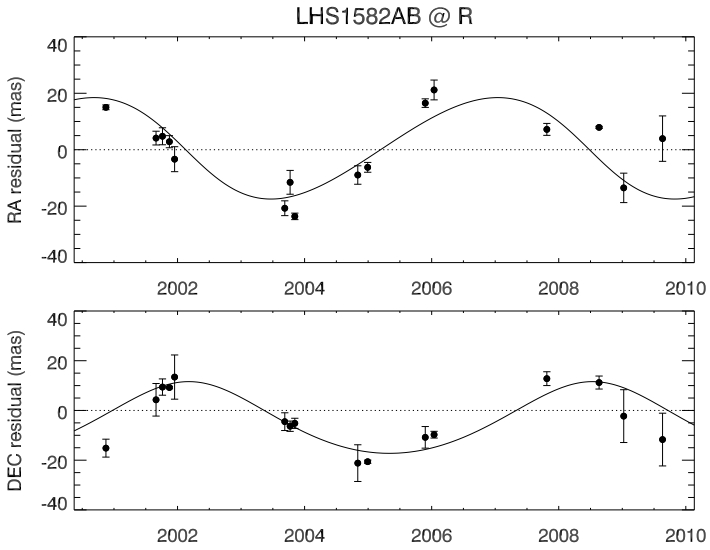

Fig. 2.— Plots of the nightly means of our astrometric residuals in RA and DEC for LHS 1582AB after solving for parallax and proper motion. A perturbation with a ∼6 year period is evident, and the resultant orbital fit (Table 5) is plotted on this graph. Two nights with only a single CCD image each (obtained for photometry) are not shown or used in the orbital solution.

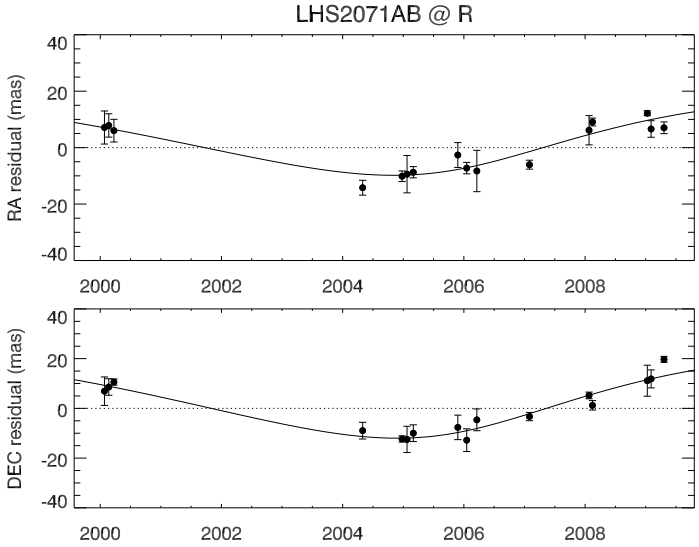

Fig. 3.— Plots of the nightly means of our astrometric residuals in RA and DEC for LHS 2071AB after solving for parallax and proper motion. A perturbation is evident, but the orbit has not wrapped in our data so the plotted orbital fit (Table 5) is poorly determined.

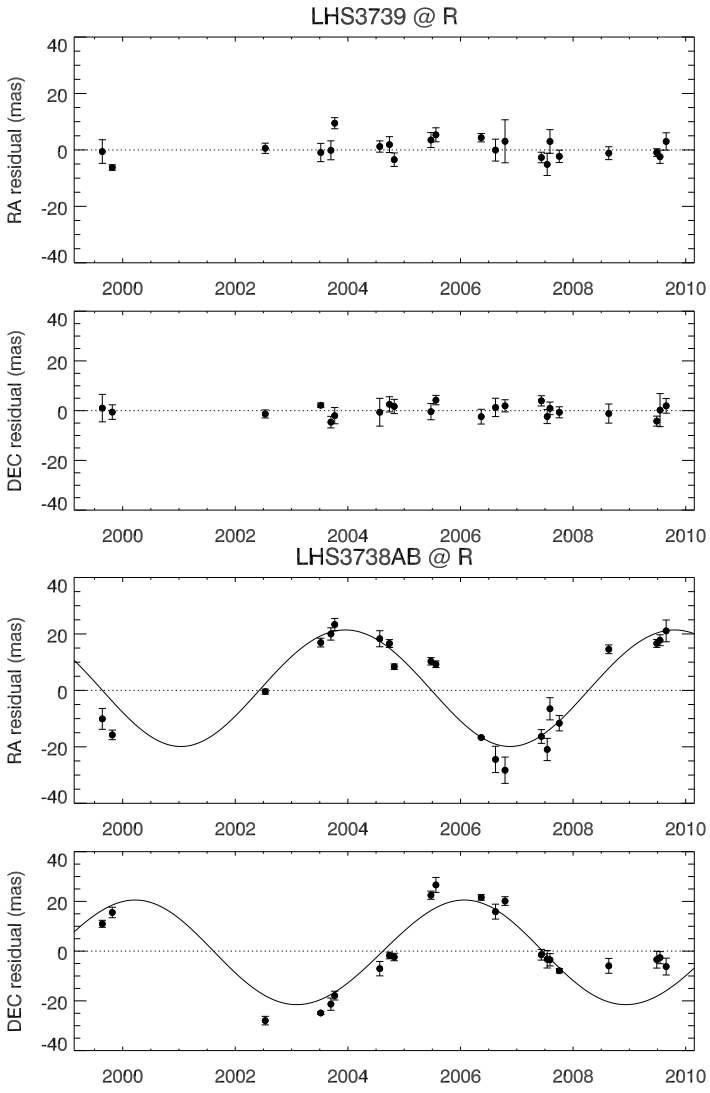

Fig. 4.— Plots of the nightly means of our astrometric residuals in RA and DEC for LHS 3739 (top) and LHS 3738AB (bottom) after solving for parallax and proper motion. LHS 3738AB clearly shows a perturbation with a period of ∼6 years whose orbital fit (Table 5) is overplotted; using the same CCD frames and reference stars the residuals for LHS 3739 remain flat. Two nights with only a single CCD image each (obtained for photometry) are not shown or used in the orbital solution.

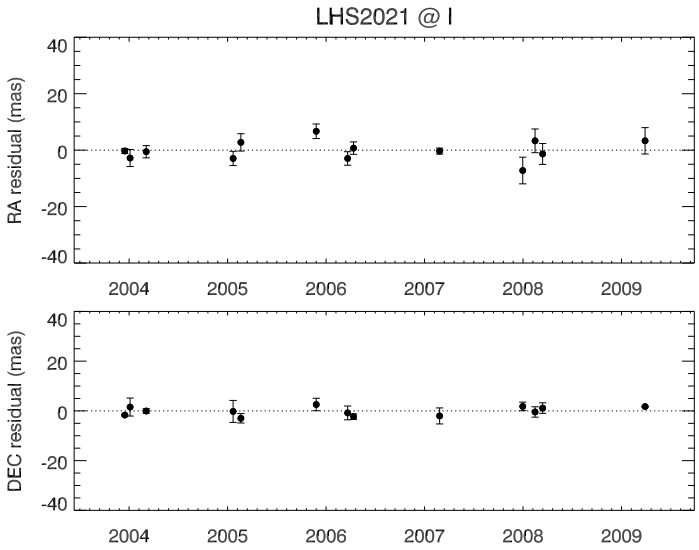

Fig. 5.— Plots of the nightly means of our astrometric residuals in RA and DEC for LHS 2021 after solving for parallax and proper motion. This star appears to a single main-sequence M dwarf. Two nights with only a single CCD image each (observed for photometry) are not shown.

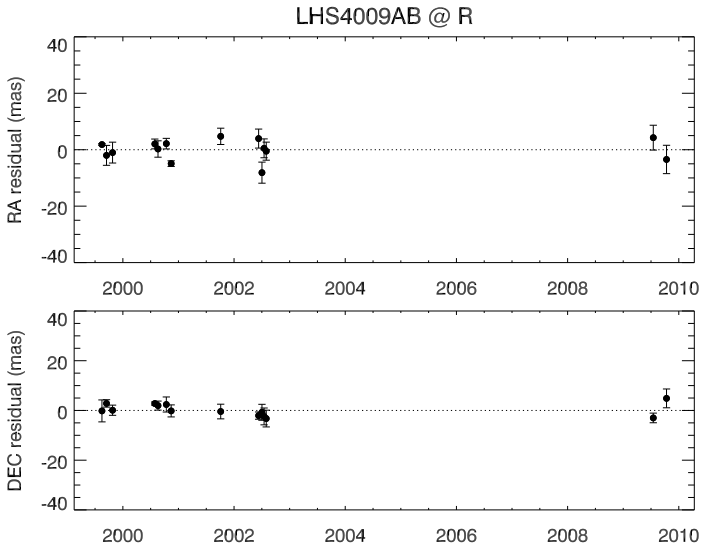

Fig. 6.— Plots of the nightly means of our astrometric residuals in RA and DEC for LHS 4009AB after solving for parallax and proper motion. There is no perturbation evident. The two components discovered in Montagnier et al. (2006) have a magnitude difference of only ΔK=0.1 and an orbital period ∼3 years. We see no evidence of duplicity in the data. One night with only a single CCD image (obtained for photometry) is not shown.

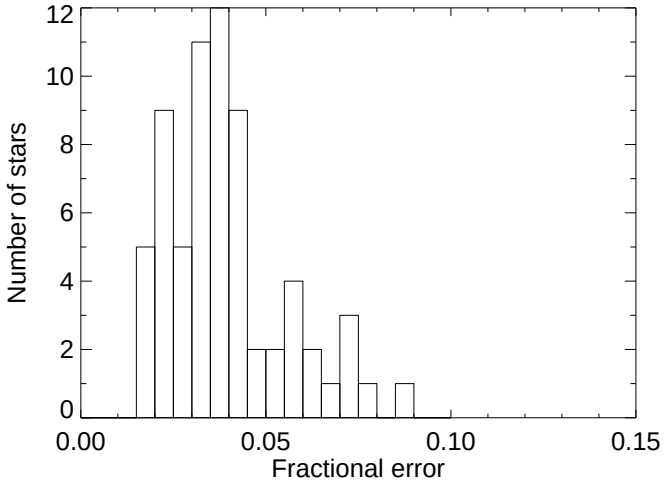

Fig. 7.— The internal photometry distance errors are shown without the 15.3% external systematic error. The average error is 3.9%, indicating that the distance estimates are remarkably consistent for this sample.

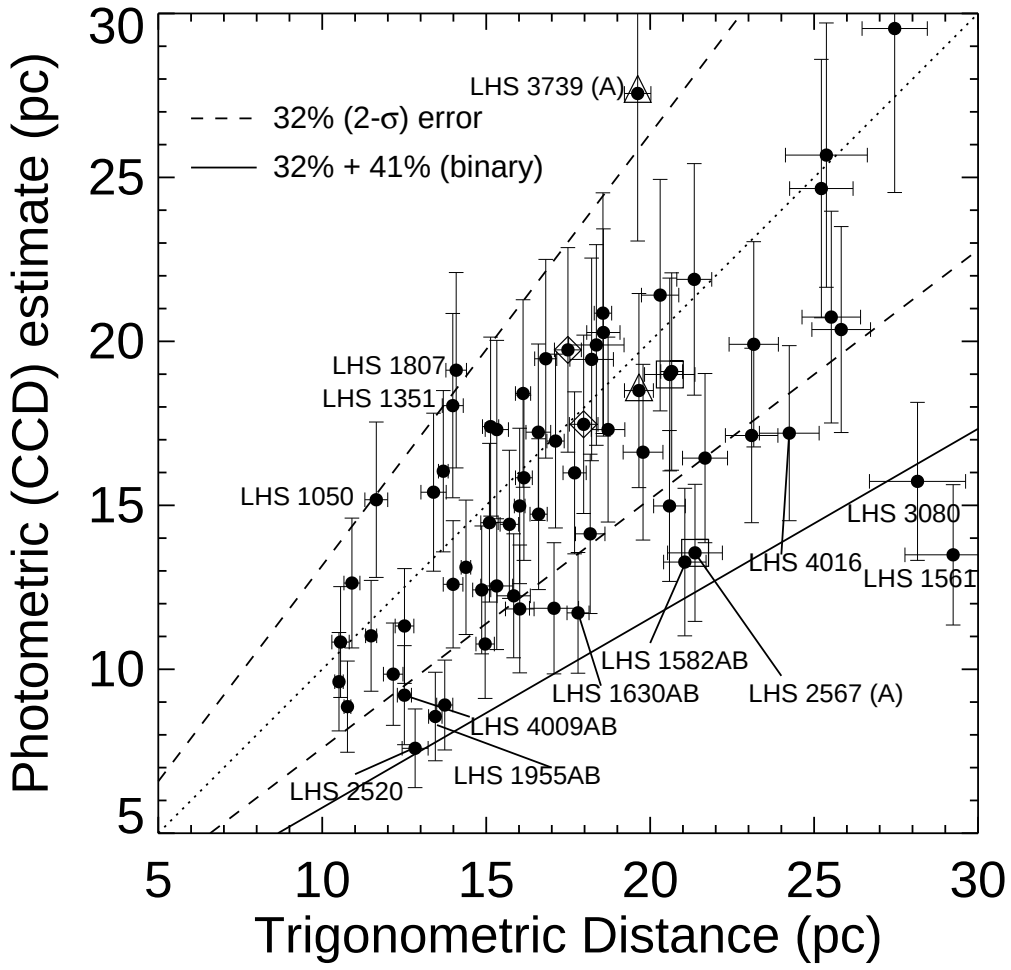

Fig. 8.— Photometric distance estimates compared to trigonometric parallax distances, identical distances are plotted with a dotted line. Dashed lines display the average 2-σ error of our photometric distance estimates. Beyond the solid line, even an equal-luminosity binary cannot fully account for the mismatch between trigonometric and photometric distance estimates. LHS 2567/2568 are plotted with squares, LHS 3001 (the nearer one by trigonometric parallax)/3002 with diamonds, and LHS 3739/3738AB with triangles. LTT 5066 at 46 pc is not plotted.

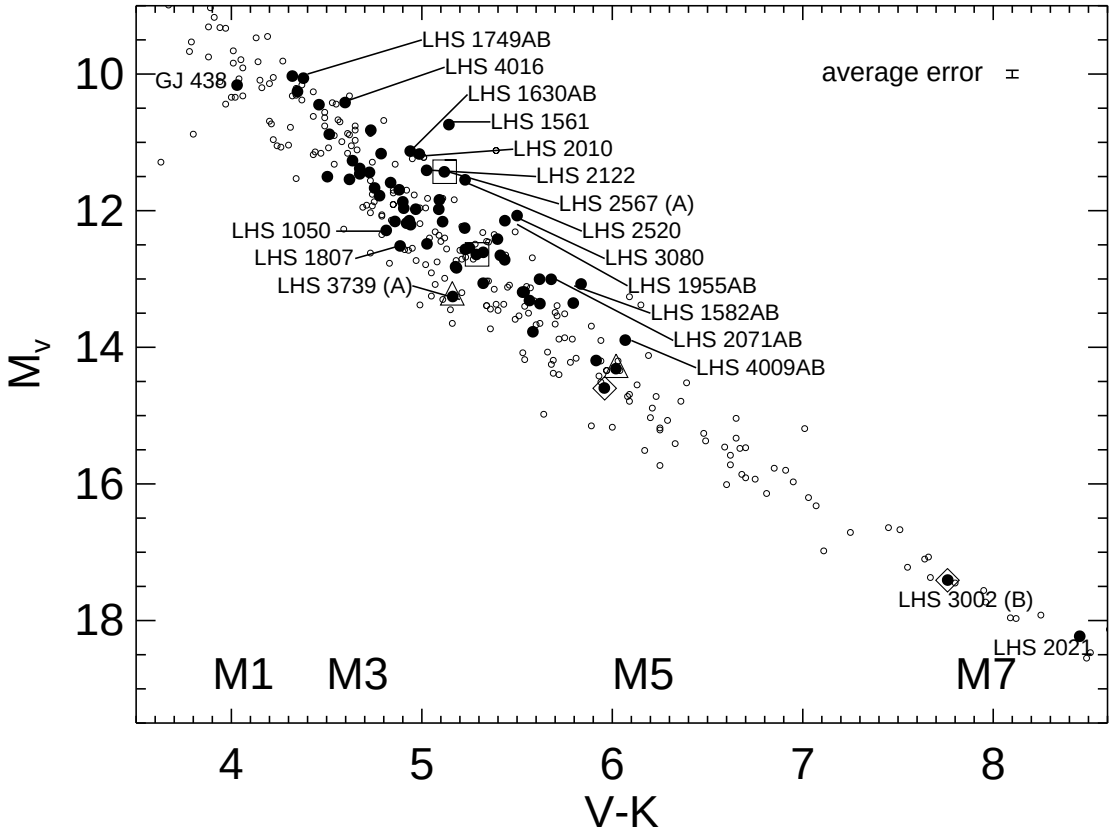

Fig. 9.— All 67 system components with parallaxes reported here are plotted as large solid points on an observational HR diagram. Small points represent stars in the RECONS 10 pc sample. LHS 2567/2568 are enclosed with squares, LHS 3001/3002 with diamonds, and LHS 3739/3738AB with triangles.

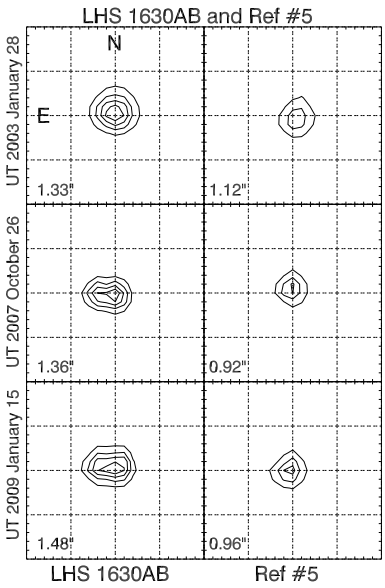

Fig. 10.— Contour plots of LHS 1630AB (left) and example single star Ref #5 (right, contours exaggerated 20 times) on three different nights in the I filter. LHS 1630B was first reported by Beuzit et al. (2004) at separation 0.″61, angle 72 deg in 2002. Grid markings are 5 pixels (2.″05), FWHM values for the PSFs are given in the lower left of each panel.

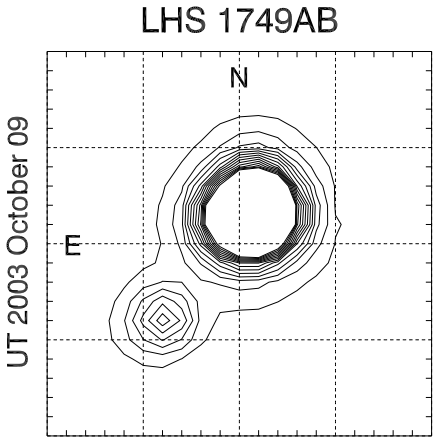

Fig. 11.— Contour plot of LHS 1749AB in the V filter on 2003 October 09. The B component is obvious in the image but difficult to separate cleanly on most frames. The four years of available data suggest slight orbital motion. Grid markings are 5 pixels (2.05″).

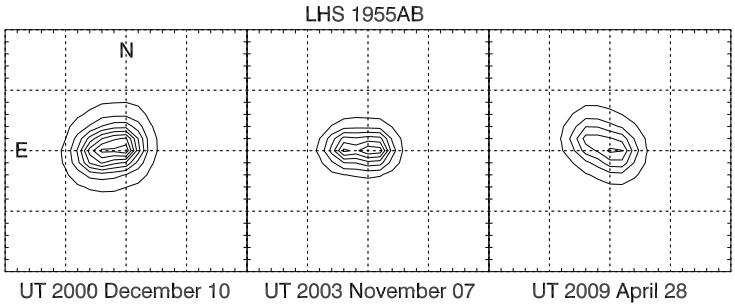

Fig. 12.— Contour plots of LHS 1955AB for three nights in the R filter. LHS 1955B is occasionally visible as a saddle point or even a peak (middle frame). The motion seen here suggests an ∼80 yr orbit. Grid markings are 5 pixels (2.05″).

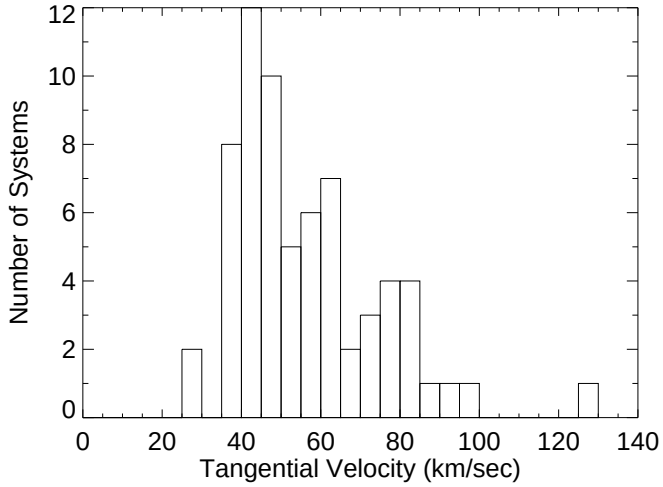

Fig. 13.— Tangential velocity distribution for our systems. The fastest moving star is also our most distant, LTT 5066.

Table 1. Astrometric Results

Name	R.A. Decl. (J2000.0)[a]	Filter	N_{sea} [b]	N_{frm}	Coverage[b]	Years [b]	N_{ref}	π(rel) (mas)	π(corr) (mas)	π(abs) (mas)	μ (mas yr^{-1})	P.A. (deg)	V_{tan} (km s^{-1})	Notes
(1)	(2) (3)	(4)	(5)	(6)	(7)	(8)	(9)	(10)	(11)	(12)	(13)	(14)	(15)	(16)
LHS 1050	00 15 49.25 +13 33 22.3	V	7s	60	1999.71–2009.75	10.03	7	84.46±2.56	1.39±0.22	85.85±2.57	699.2±0.5	061.7±0.08	38.6	c
LHS 1351	02 11 18.06 -63 13 41.0	V	3c+	68	2000.58–2004.97	4.40	5	70.62±1.64	0.91±0.09	71.53±1.64	764.6±1.3	243.2±0.18	50.7	
LHS 1358	02 12 54.63 +00 00 16.8	R	5s	58	1999.71–2003.86	4.15	5	64.09±2.07	1.18±0.13	65.27±2.07	558.3±1.3	086.1±0.20	40.5	
LHS 1491	03 04 04.49 -20 22 43.0	V	5s	70	1999.71–2005.00	5.29	9	66.32±1.24	0.96±0.16	67.28±1.25	685.4±0.7	135.2±0.12	48.3	
LHS 1582AB	03 43 22.08 -09 33 50.9	R	9s	70	2000.87–2009.63	8.76	6	45.50±1.43	1.99±0.28	47.49±1.46	506.2±0.5	052.3±0.10	50.5	c d
LHS 1630AB	04 07 20.50 -24 29 13.7	V	10s	137	1999.71–2009.03	9.32	5	54.44±1.04	1.74±0.20	56.18±1.06	683.1±0.4	163.7±0.05	57.6	c e
LHS 1748	05 15 46.72 -31 17 45.3	V	5c	58	2000.88–2005.14	4.26	9	41.76±1.40	1.42±0.05	43.18±1.40	551.6±1.1	062.6±0.22	60.6	
LHS 1749A	05 16 00.39 -72 14 12.6	V	5s	91	2000.88–2005.05	4.17	6	44.93±1.46	1.21±0.08	46.14±1.46	814.2±1.1	356.4±0.12	83.6	c g
LHS 1767	05 31 04.33 -30 11 44.8	V	5c	57	2003.96–2007.99	4.03	10	64.53±1.51	0.73±0.05	65.26±1.51	580.1±1.1	143.8±0.22	42.1	e
WT 178	05 37 39.77 -61 54 43.8	R	5s+	68	1999.91–2003.77	3.86	10	60.53±0.89	1.49±0.09	62.02±0.89	502.9±0.9	015.8±0.19	38.4	
APMPM J0544-4108	05 43 46.56 -41 08 08.4	V	5c	76	2000.14–2005.05	4.91	8	47.63±0.78	0.78±0.08	48.41±0.78	601.4±0.4	165.6±0.07	58.9	
LHS 1807	06 02 22.62 -20 19 44.2	R	4c+	66	2000.88–2007.83	6.95	6	70.02±1.57	0.98±0.14	71.00±1.58	558.3±1.3	355.7±0.19	37.3	c
GJ 1088	06 10 52.89 -43 24 17.8	V	5s	51	2000.88–2005.06	4.18	6	85.44±1.27	1.59±0.19	87.03±1.28	745.5±0.8	010.6±0.11	40.6	
LHS 1932	07 36 12.03 -51 55 21.3	V	3c	93	2000.88–2003.14	2.26	9	60.91±0.98	1.01±0.09	61.92±0.98	595.1±1.2	042.8±0.22	45.6	
LHS 1955A	07 54 54.80 -29 20 56.4	R	5c	83	2000.94–2009.32	8.38	10	72.76±1.09	1.60±0.29	74.36±1.13	596.6±0.5	146.8±0.09	38.0	c g
LHS 2010	08 27 11.83 -44 59 21.1	V	4c	85	2001.14–2004.18	3.03	9	71.33±1.27	1.47±0.30	72.80±1.30	537.0±1.2	343.1±0.22	35.0	c
LHS 2021	08 30 32.57 +09 47 15.5	I	6s+	54	2003.94–2009.24	5.30	8	62.06±1.14	1.61±0.18	63.67±1.15	667.2±0.6	226.6±0.10	49.7	c
LHS 2071AB	08 55 20.25 -23 52 15.0	R	7s	69	2000.07–2009.30	9.23	11	66.16±1.25	0.65±0.08	66.81±1.25	591.5±0.3	276.5±0.06	42.0	c d
LHS 2106	09 07 02.75 -22 08 50.1	R	5s	56	2000.06–2006.04	5.97	7	65.12±1.16	1.11±0.06	66.23±1.16	505.7±0.4	215.4±0.08	36.2	
LHS 2122	09 16 25.99 -62 04 16.0	R	6s+	64	2001.15–2009.04	7.89	9	56.42±2.57	2.17±0.15	58.59±2.57	933.8±0.9	313.3±0.10	75.5	
LHS 5156	09 42 49.60 -63 37 56.1	V	4s+	60	2005.97–2009.32	3.35	9	94.42±1.17	0.73±0.07	95.15±1.17	516.6±0.9	084.5±0.15	25.7	c f
WT 244	09 44 23.73 -73 58 38.3	I	7s+	64	1999.92–2008.00	8.08	12	42.05±1.48	1.25±0.23	43.30±1.50	517.6±0.5	258.1±0.08	56.7	
LHS 2328	10 55 34.47 -09 21 25.9	R	8s	66	2001.15–2009.25	8.10	9	53.03±1.47	0.81±0.08	53.84±1.47	516.2±0.5	330.9±0.10	45.4	
LHS 2335	10 58 35.10 -31 08 38.4	V	3c	56	2001.14–2003.14	1.99	8	49.58±1.54	0.97±0.20	50.55±1.55	571.7±3.0	260.9±0.49	53.6	
LHS 2401	11 23 57.31 -18 21 48.6	V	5s	70	2001.15–2005.14	3.99	5	51.74±2.50	2.73±0.17	54.47±2.51	576.4±1.4	266.6±0.22	50.2	
GJ 1147	11 38 24.95 -41 22 32.5	R	5s+	64	2001.15–2009.04	7.89	10	65.13±1.08	0.95±0.09	66.08±1.08	942.4±0.7	274.0±0.06	67.6	
GJ 438	11 43 19.82 -51 50 25.9	V	6s+	92	2000.06–2009.32	9.26	6	89.13±2.03	2.57±0.30	91.70±2.05	857.0±0.9	129.9±0.12	44.3	c e
LHS 2520	12 10 05.59 -15 04 16.9	V	4s	56	2000.07–2004.43	4.37	7	77.11±2.40	0.82±0.17	77.93±2.41	718.6±1.6	183.5±0.18	43.7	
GJ 1157	12 23 01.43 -46 37 08.4	V	5s	61	2001.14–2005.14	3.99	7	61.00±0.61	1.42±0.16	62.42±0.63	819.5±0.5	245.0±0.06	62.2	
LHS 2567	12 29 54.19 -05 27 24.4	R	7s	58	2000.07–2009.03	8.96	7	45.54±1.83	1.26±0.07	46.80±1.83	611.1±0.6	241.0±0.11	61.9	c A
LHS 2568	12 29 54.66 -05 27 20.6	R	7s	58	2000.07–2009.03	8.96	7	47.29±1.81	1.26±0.07	48.55±1.81	597.8±0.6	241.5±0.11	58.4	c B
LHS 2718	13 20 03.86 -35 24 44.1	V	5s	62	2001.15–2005.14	3.99	11	72.05±0.78	0.99±0.11	73.04±0.79	961.6±0.6	241.1±0.07	62.4	
LHS 2729	13 23 38.02 -25 54 45.1	R	5s	56	2001.15–2005.09	3.94	12	70.32±1.52	1.16±0.14	71.48±1.53	633.9±1.3	249.8±0.21	42.0	

Table 1—Continued

Name	R.A. (J2000.0)[a]	Decl.	Filter	N_{sea}[b]	N_{frm}	Coverage[b]	Years[b]	N_{ref}	π(rel) (mas)	π(corr) (mas)	π(abs) (mas)	μ (mas yr^{-1})	P.A. (deg)	V_{tan} (km s^{-1})	Notes
(1)	(2)	(3)	(4)	(5)	(6)	(7)	(8)	(9)	(10)	(11)	(12)	(13)	(14)	(15)	(16)
LHS 2836	13 59 10.45	-19 50 03.4	*V*	3c+	108	2000.14–2004.18	4.04	8	91.22±0.86	1.64±0.23	92.86±0.89	573.4±1.0	252.0±0.17	29.3	
LHS 2899	14 21 15.12	-01 07 19.7	*V*	5s	45	2000.14–2005.14	4.99	8	74.00±2.15	0.66±0.05	74.66±2.15	643.5±1.4	164.4±0.21	40.9	
LHS 3001	14 56 27.16	+17 57 00.0	*I*	5s	78	2000.58–2009.25	8.67	9	56.36±1.34	0.81±0.07	57.17±1.34	982.4±0.8	301.2±0.09	81.5	[c] A
LHS 3002	14 56 27.79	+17 55 08.9	*I*	5s	78	2000.58–2009.25	8.67	9	54.83±1.35	0.81±0.07	55.64±1.35	987.8±0.8	301.5±0.09	84.2	[c] B
LHS 3167	16 13 05.93	-70 09 08.0	*R*	6s	85	2000.57–2009.32	8.75	10	58.22±0.93	2.03±0.21	60.25±0.95	607.1±0.5	202.1±0.08	47.8	
LHS 3169	16 14 21.93	-28 30 36.7	*V*	5s	53	2000.58–2004.45	3.87	10	52.03±1.45	1.40±0.17	53.43±1.46	523.9±1.0	230.8±0.22	46.5	
LHS 3197	16 26 48.12	-17 23 34.3	*R*	4c+	51	2000.23–2006.37	6.14	9	53.53±1.27	1.50±0.50[h]	55.03±1.36	522.2±1.0	219.0±0.22	45.0	[c]
LHS 3218	16 35 24.64	-27 18 54.7	*R*	6s	77	2000.23–2009.32	9.09	8	51.31±0.74	2.57±0.23	53.88±0.77	889.0±0.3	180.7±0.03	78.2	
GJ 633	16 40 45.26	-45 59 59.3	*V*	7s+	100	1999.64–2007.44	7.80	10	56.88±1.05	2.59±0.56	59.47±1.19	527.2±0.4	137.4±0.09	42.0	[c] [e]
LHS 3295	17 29 27.34	-80 08 57.4	*V*	5s	68	2000.57–2004.25	3.68	8	78.20±1.79	1.75±0.33	79.95±1.82	701.7±1.5	312.8±0.25	41.6	
WT 562	18 26 19.80	-65 47 41.1	*I*	4c+	80	2000.58–2005.64	5.06	7	57.53±0.90	0.90±0.07	58.43±0.90	610.8±1.1	180.9±0.15	49.6	[c]
LHS 3413	18 49 51.21	-57 26 48.6	*R*	5s	69	2000.57–2009.32	8.75	9	81.13±2.01	1.08±0.08	82.21±2.01	675.7±0.8	254.9±0.12	39.0	
LHS 3443	19 13 07.96	-39 01 53.8	*V*	5s	69	2000.58–2009.75	9.17	8	47.44±1.14	1.13±0.10	48.57±1.14	509.2±0.5	118.3±0.10	49.7	
LHS 3583	20 46 37.08	-81 43 13.7	*V*	8s	68	2000.58–2009.32	8.75	9	93.12±2.37	1.60±0.21	94.72±2.38	764.6±1.0	135.0±0.15	38.3	[e]
APMPM J2127-3844	21 27 04.58	-38 44 50.8	*R*	4s	58	1999.62–2004.73	5.11	8	48.76±1.38	0.49±0.03	49.25±1.38	897.2±0.8	141.6±0.10	86.3	
WT 795	21 36 25.30	-44 01 00.2	*V*	4c+	74	2000.41–2004.44	4.03	5	68.84±0.69	0.69±0.12	69.53±0.70	827.0±0.6	144.4±0.08	56.4	
LHS 3719	21 49 25.91	-63 06 51.9	*V*	4s+	70	2000.58–2003.69	3.11	8	59.05±1.37	1.23±0.08	60.28±1.37	537.2±1.2	032.2±0.24	42.2	
LHS 3738AB	21 58 49.13	-32 26 25.5	*R*	9s	113	1999.64–2009.65	10.01	10	49.60±1.14	1.27±0.07	50.87±1.14	537.3±0.5	228.8±0.08	50.1	[c] BC[d]
LHS 3739	21 58 50.19	-32 28 17.8	*R*	9s	113	1999.64–2009.65	10.01	10	49.70±1.05	1.27±0.07	50.97±1.05	535.5±0.3	229.2±0.07	49.8	[c] A
WT 870	22 06 40.68	-44 58 07.4	*R*	6s	70	2000.41–2005.90	5.48	7	55.41±1.13	1.10±0.05	56.51±1.13	736.3±0.7	219.6±0.11	61.8	
LHS 3909	23 12 11.30	-14 06 11.9	*R*	3c+	55	2000.58–2007.55	6.97	6	53.41±2.00	1.49±0.05	54.90±2.00	716.3±1.7	196.0±0.24	61.8	
LHS 3925	23 17 50.33	-48 18 47.2	*R*	4c	62	2000.58–2005.80	5.23	10	45.38±1.17	1.47±0.08	46.85±1.17	755.5±0.6	157.5±0.08	76.4	
LHS 4009AB	23 45 31.26	-16 10 20.1	*R*	6s	83	1999.62–2009.78	10.15	7	79.38±1.37	0.59±0.03	79.97±1.37	690.7±0.4	216.9±0.07	40.9	[c]
LHS 4016	23 48 36.06	-27 39 38.9	*V*	6s	68	2000.87–2009.75	8.87	6	40.75±1.54	0.50±0.19	41.25±1.55	595.3±0.4	246.2±0.08	68.5	[c]
LHS 4021	23 50 31.64	-09 33 32.6	*V*	4s+	60	2000.71–2004.89	4.18	6	61.48±1.70	0.93±0.04	62.41±1.70	758.1±1.4	121.7±0.20	57.6	
LHS 4058	23 59 51.38	-34 06 42.5	*V*	5s+	59	2000.41–2006.87	6.45	7	61.15±1.98	1.99±0.38	63.14±2.02	939.0±1.2	132.8±0.15	70.5	[e]
Beyond 25 pc															
LHS 1561	03 34 39.63	-04 50 33.3	*V*	6c	61	2000.07–2009.99	9.93	9	33.19±1.72	1.01±0.11	34.20±1.72	513.0±0.7	126.6±0.16	71.1	[c]
LHS 1656	04 18 51.03	-57 14 01.1	*I*	5c+	51	2003.95–2009.74	5.78	8	38.16±1.94	1.25±0.08	39.41±1.94	814.5±1.3	022.1±0.16	98.0	
LTT 5066	13 13 29.63	-32 27 05.3	*R*	6s+	69	2000.14–2009.32	9.18	8	20.61±0.92	0.98±0.04	21.59±0.92	575.9±0.4	267.6±0.05	126.4	
LHS 3080	15 31 54.17	+28 51 09.7	*R*	6c	66	2000.58–2009.57	8.99	9	34.73±1.85	0.79±0.06	35.52±1.85	538.8±0.7	274.4±0.11	71.9	[c]
LHS 3147	16 02 23.57	-25 05 57.3	*R*	5s+	72	2001.21–2009.31	8.10	8	37.19±1.35	1.99±0.22	39.18±1.37	666.3±0.6	202.3±0.09	80.6	
GJ 762	19 34 36.48	-62 50 38.6	*V*	4c	74	2000.58–2003.30	2.72	10	37.20±1.34	1.52±0.10	38.72±1.34	510.7±1.5	227.2±0.34	62.5	

Table 1—Continued

Name	R.A. Decl. (J2000.0)[a]	Filter	N_{sea}[b]	N_{frm}	Coverage[b]	Years[b]	N_{ref}	π(rel) (mas)	π(corr) (mas)	π(abs) (mas)	μ (mas yr^{-1})	P.A. (deg)	V_{tan} (km s^{-1})	Notes
(1)	(2) (3)	(4)	(5)	(6)	(7)	(8)	(9)	(10)	(11)	(12)	(13)	(14)	(15)	(16)
LHS 3484	19 47 04.49 -71 05 33.1	*R*	7s	65	2000.58–2009.32	8.75	8	37.51±1.51	2.14±0.15	39.65±1.52	649.8±0.6	172.9±0.09	77.7	
LHS 3836	22 38 02.92 -65 50 08.8	*R*	5s	61	1999.62–2004.45	4.82	7	35.90±1.32	0.52±0.02	36.42±1.32	693.9±1.0	118.9±0.17	90.3	

[a]coordinates are epoch and equinox 2000.0; each target's coordinates were extracted from 2MASS and then transformed to epoch 2000.0 using the proper motions and position angles listed here.

[b]'Coverage' and 'Years' run from the first to last data point; 'Seasons' counts observing semesters where a dataset was taken, and denotes if coverage was 'c'ontinuous (more than one night of data in all seasons) or 's'cattered. Coverage extended by a single frame is denoted with a + in the Seasons column.

[c]System has notes in §5.

[d]The astrometric perturbation was removed from the final parallax fit.

[e]Astrometric results use new *V* filter data.

[f]Astrometric results use new *V* filter data *only*.

[g]Parallax measured for the A component alone.

[h]Generic correction to absolute adopted; field is reddened by a nebula.

Table 2. Photometric Results

Name (1)	Alternate Name (2)	V_J (3)	R_{KC} (4)	I_{KC} (5)	No. of abs. Nights (6)	π filter[a] (7)	σ (mag) (8)	No. of rel. Nights (9)	No. of Frames (10)	J (2MASS) (11)	H (2MASS) (12)	K (2MASS) (13)	spectral type (14)	ref (15)	phot dist (16)	No. of Relations (17)	Notes (18)
LHS 1050	GJ 12	12.62	11.46	10.04	3	V	.011	12	60	8.62	8.07	7.81	M3.0V	.....	15.17±2.37	12	
LHS 1351	L 125-51	12.23	11.15	9.82	2	V	.010	12	68	8.54	7.98	7.73	M2.5V	Haw96[b]	18.04±2.81	12	
LHS 1358	G 159-46	13.58	12.31	10.66	2	R	.015	11	58	9.06	8.52	8.17	M4.0V	Rei95[c]	12.54±1.94	12	
LHS 1491	LP 771-77	12.84	11.65	10.13	2	V	.018	15	70	8.63	8.02	7.75	M3.5V	Rei95	12.42±1.95	12	
LHS 1582AB	G 160-19	14.69	13.33	11.60	4	R	.019	19	70	9.80	9.18	8.85	M4.5V	Rei95	13.27±2.25	12	
LHS 1630AB	LP 833-42	12.38	11.22	9.68	4	V	.015	22	137	8.24	7.68	7.44	M3.5VJ	.....	11.72±1.84	12	a
LHS 1748	L 521-2	12.08	11.06	9.83	2	V	.017	11	58	8.59	7.99	7.73	M2.5V	Haw96	19.91±3.13	12	
LHS 1749A	L 57-44	11.74	10.70	9.47	2	V	.028	16	91	8.21	7.62	7.36	M2.0V	Haw96	16.44±2.58	12	
LHS 1767	LP 892-51	13.11	11.93	10.45	2	V	.012	13	57	9.05	8.49	8.19	M3.0V	.....	17.31±2.72	12	a
WT 178		14.81	13.47	11.77	3	R	.014	16	68	10.14	9.53	9.23	M4.5V	Rei07[d]	18.41±2.86	12	
APMPM J0544-4108		14.12	12.85	11.25	2	V	.010	17	76	9.74	9.16	8.87	M3.5V	.....	19.08±3.01	12	
LHS 1807	LP 779-10	13.26	12.10	10.62	2	R	.008	12	66	9.22	8.67	8.37	M3.0V	Kir95[e]	19.12±2.98	12	
GJ 1088	LHS 1831	12.28	11.11	9.61	2	V	.016	13	51	8.17	7.58	7.31	M3.5V	.....	11.02±1.69	12	
LHS 1932	L 240-16	12.48	11.36	9.92	2	V	.010	16	93	8.55	8.04	7.76	M3.5V	Haw96	15.84±2.52	12	
LHS 1955AB	L 601-78	12.79	11.52	9.89	2	R	.011	15	83	8.31	7.69	7.35	M4.0V	Rei95	8.56±1.35	12	
LHS 2010	L 387-102	11.86	10.70	9.19	3	V	.011	14	85	7.75	7.15	6.87	M3.5V	Haw96	8.91±1.37	12	
LHS 2021	LP 485-17	19.21	16.94	14.66	3	I	.016	15	54	11.89	11.17	10.76	M6.0V	.....	14.42±2.26	12	
LHS 2071AB	LP 844-28	13.88	12.55	10.82	3	R	.016	16	69	9.11	8.54	8.20	M4.0VJ	.....	10.77±1.66	12	
LHS 2106	LP 845-23	14.21	12.87	11.13	3	R	.014	12	56	9.53	9.00	8.65	M4.5V	Rei95	14.47±2.42	12	
LHS 2122	L 140-119	12.57	11.43	9.94	2	R	.015	11	64	8.47	7.83	7.55	M3.5V	Haw96	11.86±2.00	12	
LHS 5156	L 140-289	13.30	11.98	10.28	4	V	.010	14	60	8.62	8.10	7.77	M4.5V	.....	9.62±1.50	12	a
WT 244		15.17	13.80	12.02	3	I	.010	14	64	10.23	9.71	9.38	M4.5V	.....	17.13±2.66	12	
LHS 2328	G 163-23	13.55	12.37	10.86	2	R	.020	15	66	9.42	8.87	8.61	M3.5V	Rei95	20.27±3.16	12	
LHS 2335	LP 905-36	11.93	10.90	9.63	2	V	.010	9	56	8.36	7.76	7.47	M2.5V	Haw96	16.62±2.68	12	
LHS 2401	L 755-53	13.10	11.97	10.54	3	V	.014	12	70	9.17	8.59	8.32	M3.0V	Rei95	19.89±3.06	12	
GJ 1147	LHS 2435	13.72	12.49	10.91	3	R	.014	14	64	9.44	8.86	8.54	M3.0V	Haw96	17.40±2.73	12	
GJ 438	LHS 2447	10.35	9.36	8.27	4	V	.008	14	92	7.14	6.58	6.32	M1.0V	.....	12.63±1.98	12	a
LHS 2520	LP 734-32	12.09	10.88	9.30	3	V	.014	10	56	7.77	7.14	6.86	M3.5V	Rei95	7.59±1.20	12	
GJ 1157	LHS 2552	13.59	12.35	10.71	2	V	.010	13	61	9.17	8.63	8.36	M4.0V	Haw96	14.98±2.37	12	
LHS 2567	G 13-44A	13.08	11.87	10.33	3	R	.015	12	58	8.82	8.27	7.96	M3.5V	Rei95	13.55±2.09	12	A
LHS 2568	G 13-44B	14.21	12.96	11.37	3	R	.013	12	58	9.79	9.24	8.92	M3.5V	Rei95	18.99±2.94	12	B
LHS 2718	L 473-1	12.84	11.70	10.24	3	V	.012	12	62	8.83	8.25	7.98	M3.0V	Haw96	16.04±2.46	12	
LHS 2729	L 617-35	12.89	11.68	10.14	2	R	.012	9	56	8.66	8.07	7.78	M3.5V	Rei95	12.59±1.94	12	

Table 2—Continued

Name (1)	Alternate Name (2)	V_J (3)	R_{KC} (4)	I_{KC} (5)	No. of abs. Nights (6)	π filter[a] (7)	σ (mag) (8)	No. of rel. Nights (9)	No. of Frames (10)	J (2MASS) (11)	H (2MASS) (12)	K (2MASS) (13)	spectral type (14)	ref (15)	phot dist (16)	No. of Relations (17)	Notes (18)
LHS 2836	L 763-63	12.88	11.60	9.90	3	V	.013	22	108	8.33	7.76	7.44	M4.0V	.....	8.86±1.39	12	
LHS 2899	G 124-27	13.12	11.92	10.39	3	V	.016	12	45	8.95	8.39	8.09	M3.5V	Rei95	15.40±2.41	12	
LHS 3001	LP 441-33	15.81	14.35	12.52	2	I	.013	17	78	10.74	10.15	9.85	M4.5V	Rei95	19.74±3.12	12	A
LHS 3002	LP 441-34	18.68	16.65	14.42	2	I	.012	17	78	11.98	11.30	10.92	M6 V	Rei95	17.47±2.72	12	B
LHS 3167	L 74-208	13.71	12.45	10.82	3	R	.014	17	85	9.26	8.74	8.39	M4.0V	.....	14.73±2.30	12	
LHS 3169	L 626-41	12.95	11.80	10.29	2	V	.011	10	53	8.92	8.36	8.11	M3.5V	Rei95	17.31±2.82	12	
LHS 3197	LP 805-10	14.30	12.93	11.16	2	R	.011	14	51	9.55	9.00	8.68	M4.5V	.....	14.13±2.43	12	
LHS 3218	LP 862-184	14.18	12.93	11.28	2	R	.016	18	77	9.78	9.27	9.00	M4.0V	Rei95	20.86±3.67	12	
GJ 633	LHS 3233	12.67	11.56	10.20	5	V	.011	20	100	8.89	8.31	8.05	M2.5V	.....	19.47±3.03	12	a
LHS 3295	L 21-3	12.18	11.02	9.53	2	V	.007	14	68	8.09	7.52	7.30	M3.0V	.....	11.32±1.75	12	
WT 562		15.36	13.93	12.13	3	I	.010	18	80	10.35	9.81	9.45	M4.5V	.....	16.96±2.65	12	
LHS 3413	L 207-41	12.68	11.44	9.88	3	R	.017	13	69	8.32	7.70	7.46	M3.5V	Haw96	9.85±1.56	12	
LHS 3443	L 491-42	12.39	11.27	9.85	3	V	.009	14	69	8.47	7.92	7.66	M2.0V	Haw96	14.98±2.30	12	
LHS 3583	L 23-30	11.50	10.39	9.02	3	V	.014	14	68	7.69	7.12	6.83	M2.5V	Haw96	10.83±1.69	12	a
APMPM J2127-3844		14.60	13.31	11.66	2	R	.015	12	58	10.03	9.56	9.28	M4.0V	.....	21.41±3.53	12	
WT 795		14.15	12.80	11.08	3	V	.015	17	74	9.46	8.83	8.53	M4.0V	.....	13.11±2.05	12	
LHS 3719	L 165-102	12.56	11.45	10.08	2	V	.012	14	70	8.74	8.12	7.89	M2.0V	Haw96	17.23±2.69	12	
LHS 3738AB	LP 930-69	15.78	14.29	12.46	3	R	.010	24	113	10.65	10.09	9.76	M4.5V	Haw96	18.50±2.96	12	BC
LHS 3739	LP 930-70	14.72	13.45	11.88	3	R	.010	24	113	10.39	9.83	9.56	M3.5V	Haw96	27.56±4.50	12	A
WT 870		14.43	13.10	11.40	2	R	.015	15	70	9.76	9.18	8.89	M4.0V	.....	15.99±2.47	12	
LHS 3909	LP 762-3	12.97	11.82	10.40	2	R	.012	12	55	9.06	8.48	8.22	M3.0V	Rei95	19.45±3.09	12	
LHS 3925	L 359-91	13.61	12.44	10.92	2	R	.008	12	62	9.53	8.97	8.71	M3.5V	Haw96	21.89±3.53	12	
LHS 4009AB	G 273-130	14.38	12.90	10.99	3	R	.017	17	83	9.21	8.61	8.31	M4.5VJ	.....	9.21±1.51	12	
LHS 4016	G 275-106	12.34	11.24	9.90	2	V	.016	16	68	8.58	8.02	7.74	M2.5V	Rei95	17.20±2.67	12	
LHS 4021	G 273-147	13.44	12.19	10.59	2	V	.017	15	60	8.94	8.39	8.04	M4.0V	Rei95	11.84±1.95	12	
LHS 4058	G 267-11	12.84	11.64	10.08	2	V	.011	16	59	8.59	7.98	7.74	M3.5V	.....	12.24±1.89	12	a
Beyond 25 pc																	
LHS 1561	G 77-64	13.07	11.84	10.30	4	V	.010	13	61	8.83	8.27	7.93	M3.5V	Rei95	13.49±2.14	12	
LHS 1656	L 178-47	13.29	12.18	10.84	2	I	.009	13	51	9.52	8.94	8.65	M2.5V	.....	25.68±4.03	12	
LTT 5066	LHS 2698	14.21	13.14	11.76	2	R	.010	16	69	10.48	9.96	9.70	M3.0V	.....	44.38±7.27	12	
LHS 3080	G 167-47	14.32	13.01	11.32	2	R	.012	17	66	9.67	9.11	8.82	M4.0V	.....	15.73±2.41	12	
LHS 3147	LP 861-12	13.20	12.09	10.63	2	R	.012	18	72	9.28	8.69	8.41	M3.5V	Rei95	20.74±3.23	12	
GJ 762	LHS 3471	12.09	11.07	9.83	2	V	.008	13	74	8.59	8.00	7.77	M2.5V	Haw96	20.36±3.14	12	

Table 2—Continued

Name (1)	Alternate Name (2)	V_J (3)	R_{KC} (4)	I_{KC} (5)	No. of abs. Nights (6)	π filter[a] (7)	σ (mag) (8)	No. of rel. Nights (9)	No. of Frames (10)	J (2MASS) (11)	H (2MASS) (12)	K (2MASS) (13)	spectral type (14)	ref (15)	phot dist (16)	No. of Relations (17)	Notes (18)
LHS 3484	L 79-24	13.88	12.70	11.19	2	R	.008	14	65	9.79	9.22	8.98	M3.5V	Haw96	24.66±3.94	12	
LHS 3836	L 119-44	14.34	13.14	11.61	2	R	.009	11	61	10.18	9.67	9.41	M3.5V	.....	29.54±5.00	12	

Note. — Photometry data collected on the sample. All data collected or calculated by CTIOPI except where otherwise noted.

[a]Astrometric results and relative photometry use new V filter data.

[b]Hawley et al. (1996)

[c]Reid et al. (1995)

[d]Reid et al. (2007) (luminosity class inferred from the paper, where giants were simply discarded)

[e]Kirkpatrick et al. (1995)

Table 3. Combined system parallaxes

Name (1)	π (mas) (2)	source (3)	Name (4)	π (mas) (5)	source (6)	Weighted π (mas) (7)
LHS 1050	85.85±2.57	this work	LHS 1050	86.60±13.40	YPC	85.88±2.52
LHS 1749A	46.14±1.46	this work	LHS 1749A	45.36±5.08	1.5m	46.08±1.40
LHS 2021	63.67±1.15	this work	LHS 2021	59.81±4.52	1.5m	63.44±1.11
GJ 438	91.70±2.05	this work	GJ 438	118.90±15.00	YPC	92.20±2.03
LHS 2567	46.80±1.83	this work	LHS 2568	48.55±1.81	this work	47.68±1.29
LHS 3001	57.17±1.34	this work	LHS 3002	55.64±1.35	this work	56.41±0.95
GJ 633	59.47±1.19	this work	GJ 633	104.00±13.70	YPC	59.80±1.19
LHS 3739	50.97±1.05	this work	LHS 3738AB	50.87±1.14	this work	50.92±0.77
GJ 762	38.72±1.34	this work	GJ 762	60.30±14.90	YPC	38.89±1.33

Note. — 'YPC' is van Altena et al. (1995); '1.5m' is the CTIOPI 1.5m program, Costa et al. (2006).

Table 4. Multiple System Parameters

Binary Name 1	UT Date 2	Sep. (mas) 3	PA (deg) 4	Period (years) 5	Δ *mag* 6	Notes 7
LHS 1582AB	-	18.4±2.8[a]	-	6.35±0.25	-	
LHS 1630AB	-	-	-	>9	-	(never resolved)
LHS 1749AB	2002 JAN 31	2847.8±28.5	138.2±0.30	>4	ΔV ∼2.8[b]	
	2004 DEC 28	2853.8±10.9	140.0±0.19			
LHS 1955AB	2001 JAN 18	808.1±31.8	103.9±4.40	∼80	ΔR ∼0.5[b]	
	2009 APR 28	948.8:	66.5:			[c]
LHS 2071AB	-	21.2±4.0[a]	-	16.46±2.83		period uncertain
LHS 2567/8	2000 JAN 27	7938.2± 3.6	61.3±0.03	>9	ΔV =1.14	
	2009 JAN 13	8062.2± 1.7	61.4±0.03			
LHS 3001/2	2000 JUL 30	12676.9± 7.3	45.4±0.02	>9	ΔV =2.96	
	2009 MAR 31	12702.6± 4.7	46.1±0.02			
LHS 3739/8	1999 OCT 26	113215.6±31.4	353.7±0.01	>10	ΔV =1.06	(wide)
	2009 AUG 27	113115.6±25.1	354.3±0.01			
LHS 3738AB	-	26.5±1.8[a]	-	5.85±0.16		(close)
LHS 4009AB	-	-	-	-	-	(never resolved)

Note. — All angles and separations measured from the A component. Separations include a 0.015% systematic error; angles include a 0.0083 degree error.

[a]Photocentric semimajor axis

[b]Estimate from relative photometry from relative parallax reduction

[c]Based on two and one frames, respectively; uses different centroiding parameters.

Table 5. Preliminary Orbital Elements

Designation 1	P (yr) 2	a[a] (arcsec) 3	i (deg) 4	Long. Nodes (Ω) (deg) 5	T (yr) 6	e 7	Long. Periastron (ω) (deg) 8
LHS 1582AB	6.4±0.2	0.018±0.003	140.8±14.1	279.7±24.0	2002.2±0.3	0.19±0.06	258.4±23.0
LHS 2071AB	16.4±2.8[b]	0.021±0.004	090.9±2.6	219.1±3.6	2005.9±1.0	0.31±0.12	33.2±26.23
LHS 3738AB	5.8±0.2	0.027±0.002	118.9±5.16	315.9± 5.5	2006.9±1.3	0.04±0.04	26.7±82.7

[a]Photocentric semimajor axis

[b]Highly uncertain

Table 6. Comparison of spectral types

Name (1)	SpType RECONS (2)	SpType PMSU (3)	Ref (4)
LHS1050	M3.0V	M3.0	1
LHS1630AB	M3.5VJ	M3.5	2
LHS1767	M3.0V	M3.5	2
LHS2071AB	M4.0VJ	M4	2
LHS2836	M4.0V	M4	2
LHS3197	M4.5V	M4.5	2
LHS3295	M3.0V	M3.5	2
LHS4009AB	M4.5VJ	M5	2
LHS4058	M3.5V	M3.0	2
LHS3080	M4.0V	M4.5	1
LHS3836	M3.5V	M3.5	2

Note. — Comparison of our spectral types versus PMSU for all overlapping systems. 1.) Reid et al. (1995) 2.) Hawley et al. (1996)